

## Supporting Information

### **A New Polar Perovskite Coordination Network with Azaspiroundecane as A-site Cation**

Stefan Burger,<sup>a</sup> Silva Kronawitter,<sup>a</sup> Hanna L. B. Boström,<sup>b</sup> Jan Zaręba<sup>c</sup> and Gregor Kieslich<sup>a</sup>

<sup>a</sup> Department of Chemistry, Technical University Munich, Lichtenbergstrasse 4, 85748 Garching, Germany.

<sup>b</sup> Department of Chemistry, Ångström Laboratory, Uppsala Universitet, Box 538, 751 21 Uppsala, Sweden.

<sup>c</sup> Advanced Materials Engineering and Modelling Group, Wrocław University of Science and Technology, Wybrzeże Wyspiańskiego 27, 50-370 Wrocław.

#### **Table of content:**

<b>Synthetic procedures .....</b>	<b>2</b>
<b>NMR Spectroscopy of the A-site precursor [ASU]Br .....</b>	<b>3</b>
<b>Thermal analysis of the coordination networks .....</b>	<b>5</b>
<b>Powder X-ray diffraction data .....</b>	<b>7</b>
<b>Single crystal X-ray diffraction data .....</b>	<b>9</b>
<b>Group theoretical analysis.....</b>	<b>13</b>
<b>Second Harmonic Generation studies.....</b>	<b>14</b>
<b>References .....</b>	<b>15</b>

## Synthetic procedures

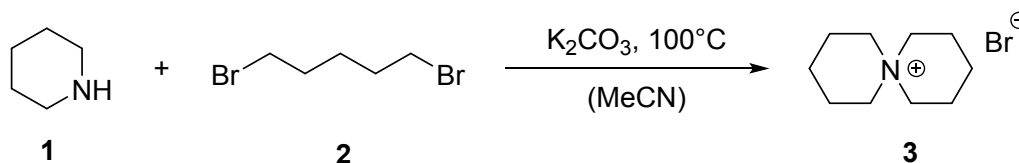
### Synthesis of 6-azaspiro[5.5]undecane bromide ([ASU]Br):

[ASU]Br was synthesised from commercially available 1,5-dibromopentane **2** and piperidine **1**. In a typical three-necked flask setup, the 1,5-dibromopentane (3.4 ml, 25 mmol) and potassium carbonate (4.15 g, 30 mmol) were mixed in acetonitrile (70 ml). After heating to reflux temperature, a solution of piperidine (2.5 ml, 25 mmol) in acetonitrile (10 ml) was added dropwise and stirred overnight, forming a white precipitate. After cooling down to room temperature, the solvent was removed under reduced pressure. The white precipitate was mixed with excess of ethanol (70 ml) and filtered to remove remaining  $K_2CO_3$ . The filtrate was concentrated in vacuo and precipitated in pure diethylether (80 ml) to yield a fine, white solid. This crude product was washed with diethylether (2 x 10 ml) and dried to constant weight, resulting in 3.9 g of pure product (67% yield) as a fine crystalline powder (see Figure S 3, 4).

**$^1H$ -NMR** (400 MHz, Deuterium Oxide):  $\delta$  [ppm] = 3.29 (t,  $J$  = 6.4 Hz, 8H), 1.89-1.67 (m, 8H), 1.58 (p,  $J$  = 6.4, 5.9 Hz, 4H).

**$^{13}C$ -NMR** (101 MHz, Deuterium Oxide):  $\delta$  [ppm] = 59.48, 21.13, 18.87.

**Figure S1:** Reaction scheme of [ASU]Br *via* a nucleophilic substitution mechanism. The route was adapted and modified from the literature.<sup>1</sup> The reaction is expected to also run under milder conditions and is flexible towards different di-haloalkanes which can be used to vary the carbon chain length in the resulting spiro compound.



### Synthesis of crystalline coordination networks:

For the preparation of the crystalline [ASU][Cd(C<sub>2</sub>N<sub>3</sub>)<sub>3</sub>] material and the other compounds for B = Mn<sup>2+</sup>, Co<sup>2+</sup>, and Ni<sup>2+</sup> commercially available Na(dca) (96%, Aldrich), Cd(Cl<sub>2</sub>)·H<sub>2</sub>O (98.5%, Alfa Aesar), Mn(NO<sub>3</sub>)·4H<sub>2</sub>O (98%, Alfa Aesar), Co(NO<sub>3</sub>)·6H<sub>2</sub>O (99%, abcr), Ni(NO<sub>3</sub>)<sub>2</sub>·6H<sub>2</sub>O (Alfa Aesar), millipore water and [ASU]Br were used. The synthesis of the coordination networks was approached *via* a mild solution chemistry procedure at ambient temperature. In a typical crystallisation approach, 0.25 ml water was placed at the bottom of a tube and then layered in order by 0.3 ml of an aqueous solution of Na(dca)

(2M), 0.5 ml of an aqueous  $M(\text{NO}_3/\text{Cl}_2) \cdot x\text{H}_2\text{O}$  solution (0.4M) and an aqueous solution of  $[\text{ASU}]\text{Br}$  (0.4M). Large block single crystals with sizes between 0.1 – 1 mm were collected after a couple of hours at ambient temperature and washed with the respective solvent.



**Figure S2:** Photographs of the resulting crystals formed, exemplarily shown here for the colorless, large block crystals of the  $[\text{ASU}][\text{Cd}(\text{C}_2\text{N}_3)_3]$  material.

## NMR Spectroscopy of the A-site precursor $[\text{ASU}]\text{Br}$

The  $^1\text{H}$ - and  $^{13}\text{C}$ -NMR spectra were recorded on a *Bruker Avance III 400* spectrometer at room temperature (298 K). Chemical shifts are expressed as parts per million (ppm,  $\delta$ ). The following abbreviations t = triplet p = pentet and m = multiple are used to characterise all signals. All coupling constants are absolute values and are expressed in Hertz (Hz).<sup>2</sup>

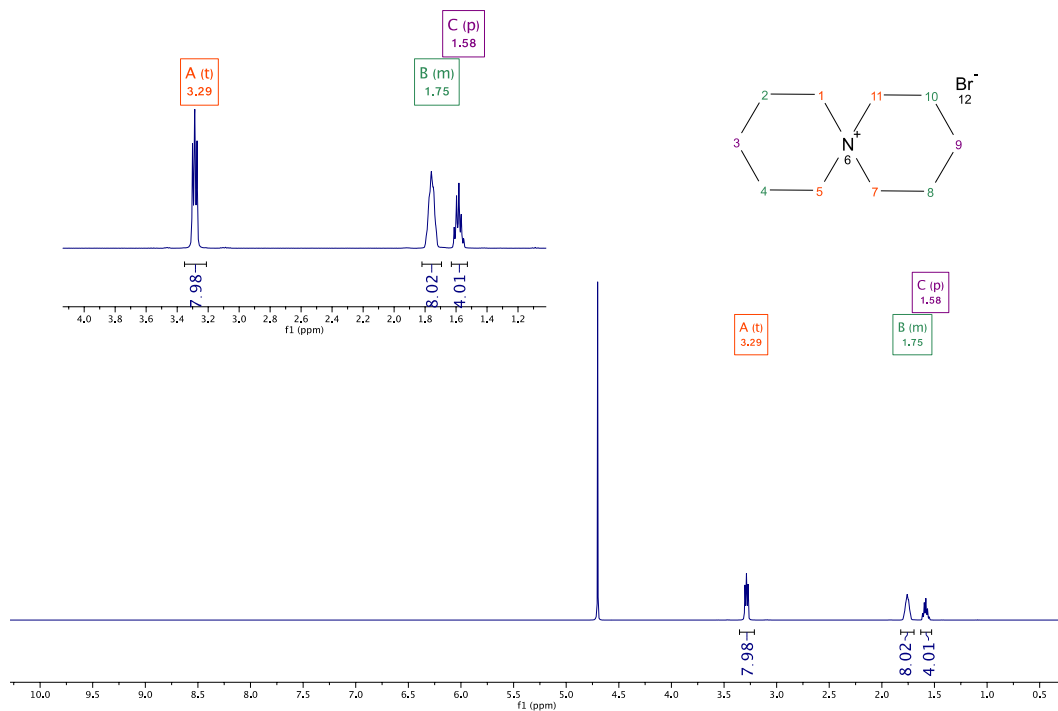


**Figure S3:**  $^1\text{H-NMR}$ -spectrum of [ASU]Br in Deuterium Oxide. All protons of the cyclic aliphatic amine could be assigned, confirming the purity of the compound.

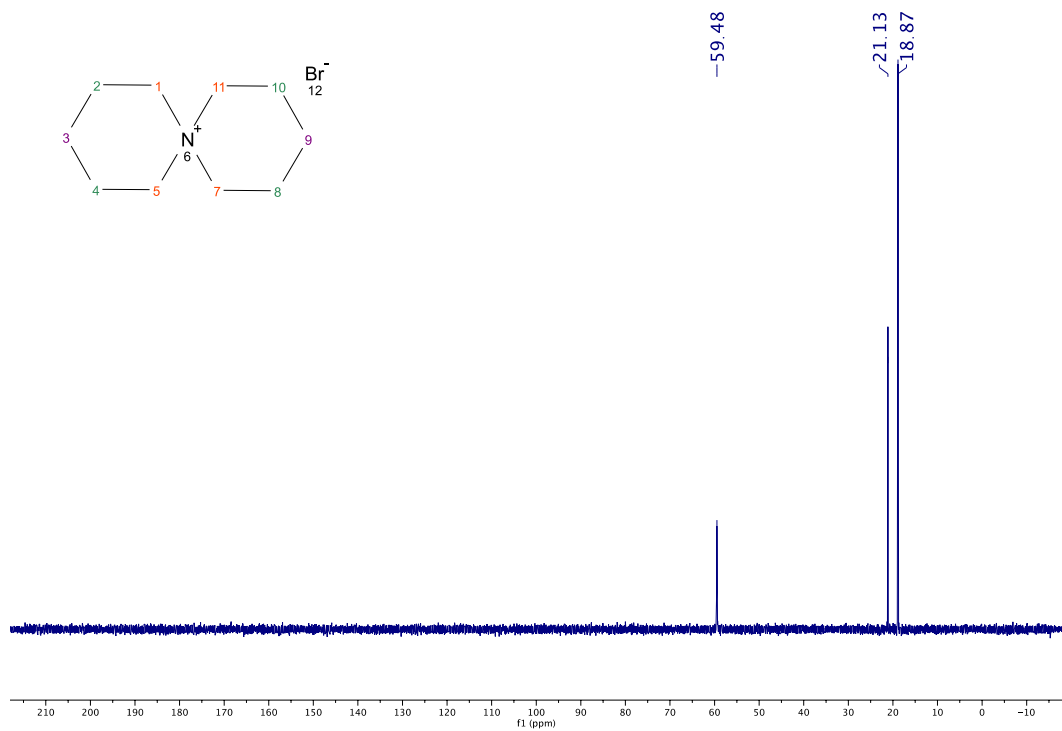


**Figure S4:**  $^{13}\text{C-NMR}$ -spectrum of [ASU]Br in Deuterium Oxide, showcasing only the three expected signals.

## Thermal analysis of the coordination networks

### Differential Scanning Calorimetry (DSC):

A DSC measurement was carried out on a DSC Q2000 from *TA instruments* with a heating rate of  $10 \text{ K min}^{-1}$  and a constant helium gas flow rate of  $25 \text{ ml min}^{-1}$ . A sample mass of  $6.7400 \text{ mg}$  was used for heating/cooling cycles. With regard to the decomposition temperature of the material, a temperature range between  $-150 \text{ }^\circ\text{C}$  and  $150 \text{ }^\circ\text{C}$  was chosen, using liquid nitrogen as cooling medium.

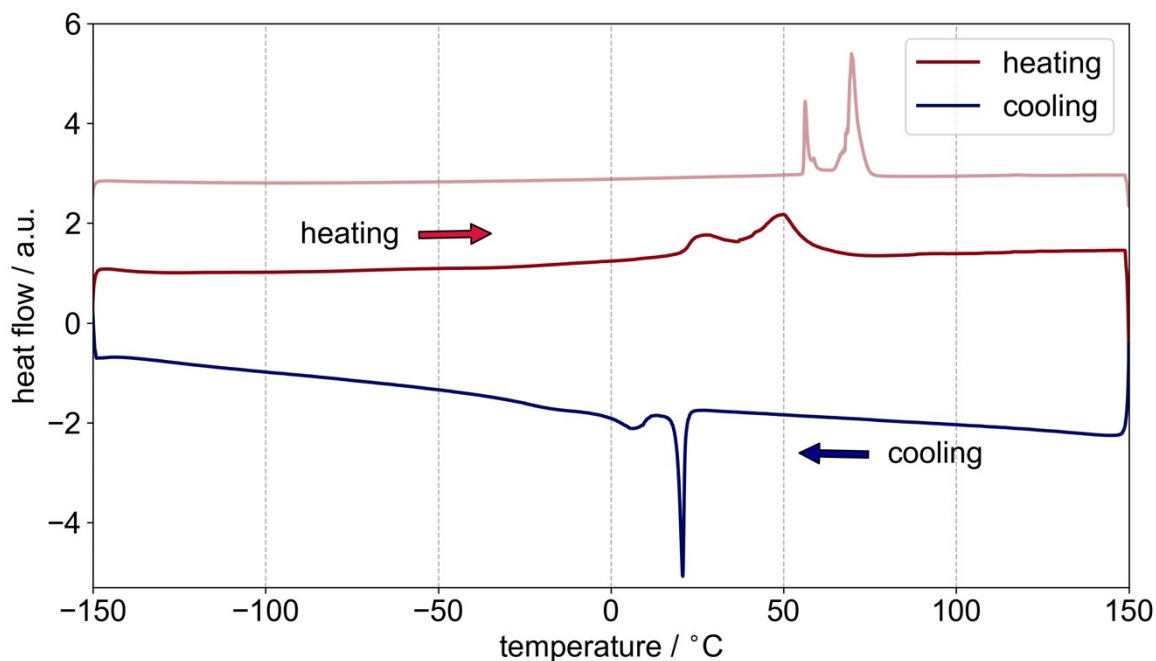


**Figure S5:** DSC curve as a function of temperature obtained by heating (red) and cooling (blue) the sample  $[\text{ASU}][\text{Cd}(\text{C}_2\text{N}_3)_3]$  at a rate of  $10 \text{ K min}^{-1}$  and a constant helium gas flow rate of  $25 \text{ ml min}^{-1}$ . An irreversible heat event during the first heating cycle at approximately  $55 \text{ }^\circ\text{C}$  is indicated by a feature, visualised by the upper light red line. During the subsequent cycles, a reproducible, reversible heat event at  $20 \text{ }^\circ\text{C}$  (heating) and  $22 \text{ }^\circ\text{C}$  (cooling) is observed. Please note, that these reversible heat event can be regarded as two distinct events, pointing at the possibility of two phase transitions with phase transition temperatures close to each other.

### Thermogravimetric analysis:

The determination of the thermal stability of the material was carried out with a *Netzsch STA 449F5* Jupiter machine using aluminum oxide pans with a sample mass of  $8.1540 \text{ mg}$ . The temperature of the oven cell was calibrated based on the melting points of the following metals: In, Sn, Bi and Zn. A baseline correction was performed by screening an empty sample pan with the respective temperature program prior to the experiment.

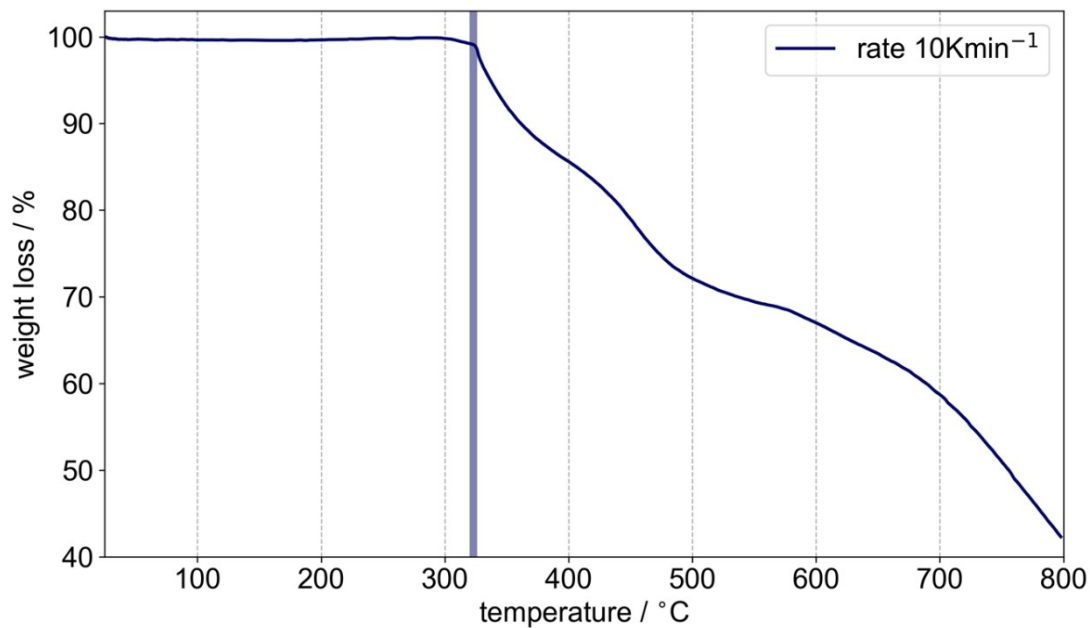


**Figure S6:** Thermal gravimetric analysis of  $[\text{ASU}][\text{Cd}(\text{C}_2\text{N}_3)_3]$  from 25 °C to 800 °C with a rate of 10 K min<sup>-1</sup>. The vertical blue line indicates the point of decomposition around 323 °C.

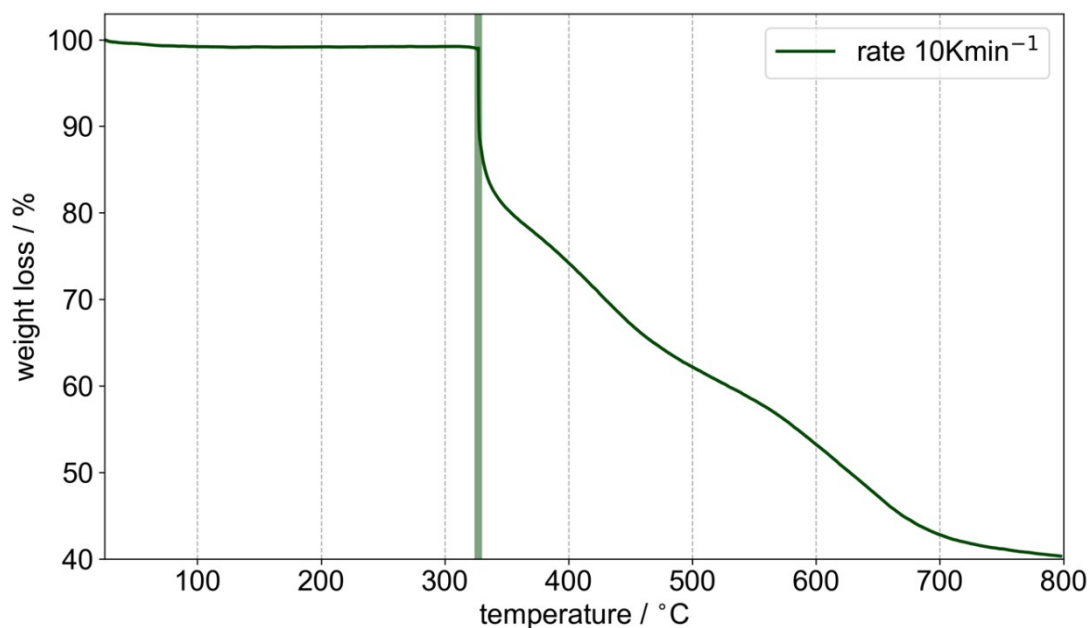


**Figure S7:** Thermal gravimetric analysis of  $[\text{ASU}]_2[\text{Ni}_2(\text{C}_2\text{N}_3)_6] \cdot 2\text{H}_2\text{O}$  from 25 °C to 800 °C with a rate of 10 K min<sup>-1</sup>. No sign for any weight loss that could potentially relate to a release of the coordinated water molecule can be observed. The vertical green line indicates the point of decomposition around 325 °C.

## Powder X-ray diffraction data

The PXRD measurements were performed using *Debye-Scherrer* geometry with borosilicate glass capillaries (0.5 mm in diameter) for the Cd perovskite compound and *Bragg-Brentano* geometry for the non-perovskite coordination networks in a PANalytical Empyrean diffractometer and a PANalytical PIXcel 1D detector with in-house Cu K<sub>α</sub> radiation ( $\lambda_1 = 1.5406 \text{ \AA}$ ,  $\lambda_2 = 1.5444 \text{ \AA}$ ,  $I_2/I_1 = 0.5$ ) operated at 45 kV (voltage) and 40 mA (intensity). A Ni-filter was used to remove the K<sub>β</sub> radiation. The measurement range was from 5.0° to 90° (2θ) for the Cd compound and from 5.0° to 50° (2θ) for the Mn, Co and Ni compounds with a minimum step size of 0.031° (2θ).

*Pawley* profile fit analysis was carried out for all patterns by using TOPAS v6. Standard deviations of all parameters were calculated and the use of "randomize\_on\_errors" ensured that the minimum of

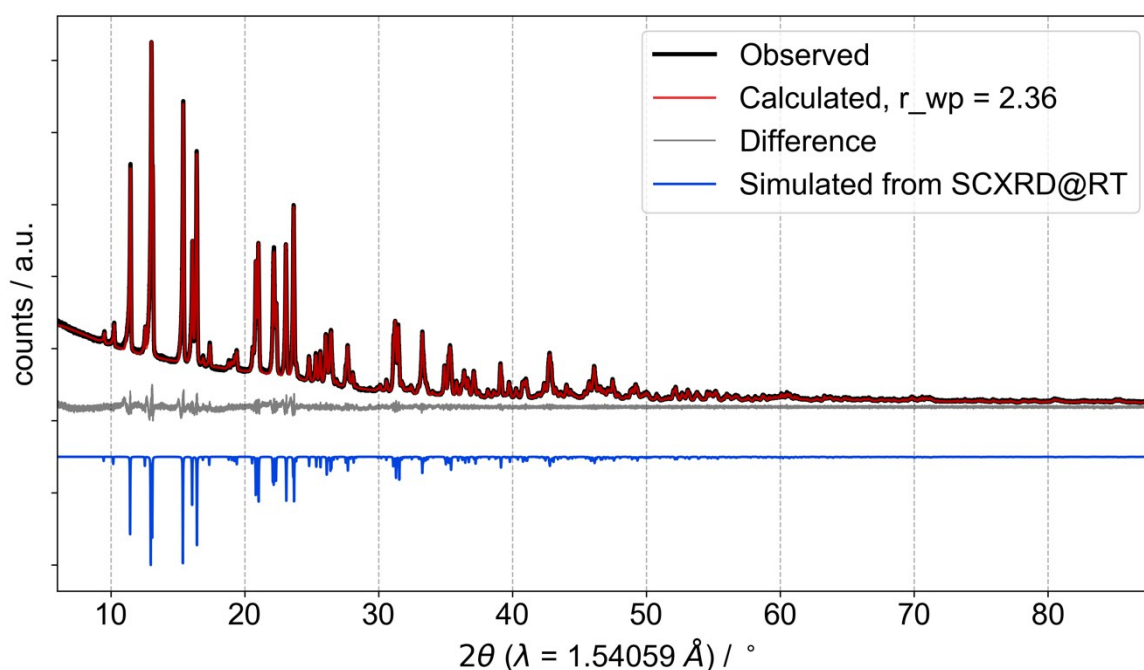


**Figure S8:** The Powder X-ray diffraction pattern of the obtained [ASU][Cd(C<sub>2</sub>N<sub>3</sub>)<sub>3</sub>] compound is shown in black, the simulated pattern from the single crystal structure at room temperature in blue and the calculated data from Pawley profile fit analysis in red, with  $r_{wp} = 2.36$ ,  $r_{exp} = 1.55$  and  $GOF = 1.52$ . The difference curve of the Pawley profile fit (grey) and the experimental data indicates the phase purity of the Cd compound.

refinement was achieved.

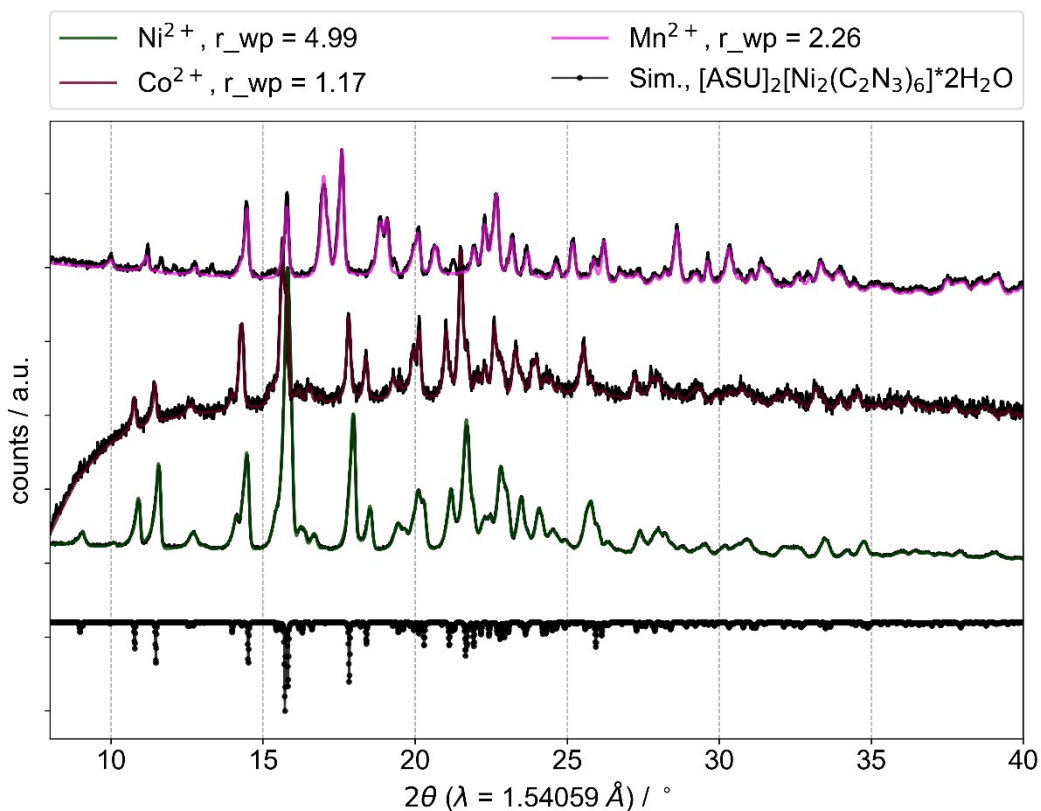


**Figure S9:** The Powder X-ray diffraction patterns of the isostructural  $[\text{ASU}]_2[\text{B}_2(\text{C}_2\text{N}_3)_6]\cdot 2\text{H}_2\text{O}$  ( $\text{B} = \text{Mn}^{2+}$ ,  $\text{Co}^{2+}$  and  $\text{Ni}^{2+}$ ) compounds are shown in pink ( $\text{B} = \text{Mn}^{2+}$ ), purple ( $\text{B} = \text{Co}^{2+}$ ) and green ( $\text{B} = \text{Ni}^{2+}$ ) and the simulated pattern from the single crystal structure of the Ni compound.

$[\text{ASU}]_2[\text{M}_2(\text{C}_2\text{N}_3)_6]\cdot 2\text{H}_2\text{O}$	$\text{M} = \text{Mn}^{2+}$	$\text{M} = \text{Co}^{2+}$	$\text{M} = \text{Ni}^{2+}$
a (Å)	19.828(6)	20.628(6)	20.508(7)
b (Å)	10.187(3)	10.009(3)	9.971(4)
c (Å)	20.599(4)	20.900(5)	20.754(7)
Beta $\beta$ (°)	105.73(1)	106.19(1)	106.18(3)
Cell volume V (Å <sup>3</sup> )	4005(2)	4144(2)	4076(2)
Space group	$P2_1/n$	$P2_1/n$	$P2_1/n$
r_wp	2.265	0.901	4.992
r_exp	1.569	1.010	1.414
GOF	1.443	0.892	3.530

**Table S1:** Comparison of the crystallographic data of the coordination networks  $[\text{ASU}]_2[\text{B}_2(\text{C}_2\text{N}_3)_6]\cdot 2\text{H}_2\text{O}$  ( $\text{B} = \text{Mn}^{2+}$ ,  $\text{Co}^{2+}$  and  $\text{Ni}^{2+}$ ), extracted from the PXRD data.

## Single crystal X-ray diffraction data

Single crystal X-Ray diffraction intensity data were collected on a *Bruker* APEX-II CCD diffractometer equipped with an fine-focus tube with a Mo K<sub>α</sub> radiation source ( $\lambda = 0.71073 \text{ \AA}$ ), a *Triumph* monochromator, a CMOS plate detector and an *Oxford Cryosystems* cooling device by using the APEX III software package.<sup>3</sup> The crystals were fixed on the top of a microsampler, transferred to the diffractometer and frozen under a stream of cold nitrogen. A matrix scan was used to determine the initial lattice parameters. Reflections were merged and corrected for Lorentz and polarization effects, scan speed, and background using SAINT.<sup>4</sup> Absorption corrections, including odd and even ordered spherical harmonics were performed using SADABS.<sup>5</sup> Space group assignments were based upon systematic absences, E-statistics, and successful refinement of the structures. Data reduction was performed with APEX3 and structure solution was performed by using SHELX<sup>6</sup> as integrated in Olex2.<sup>7</sup> Structures were solved by direct methods with the aid of successive difference Fourier maps, and were refined against all data. Hydrogen atoms were placed in calculated positions and refined using a riding model.

**Table S2:** Crystallographic data from SCXRD for the [ASU][Cd(C<sub>2</sub>N<sub>3</sub>)<sub>3</sub>] compound at 100 K.

<b>Compound</b>	[ASU][Cd(C <sub>2</sub> N <sub>3</sub> ) <sub>3</sub> ]
<b>Chemical Formula</b>	C <sub>16</sub> H <sub>20</sub> CdN <sub>10</sub>
<b>Formula weight (g/mol)</b>	464.83
<b>Temperature (K)</b>	100
<b>Crystal system</b>	orthorhombic
<b>Space group</b>	<i>Pna</i> 2 <sub>1</sub>
<b>a (Å)</b>	17.1022(9)
<b>b (Å)</b>	10.7274(5)
<b>c (Å)</b>	10.7037(5)
<b>α (°)</b>	90
<b>β (°)</b>	90
<b>γ (°)</b>	90
<b>Volume (Å<sup>3</sup>)</b>	1963.72(17)
<b>Z</b>	4
<b>ρ<sub>calc</sub> (g/cm<sup>3</sup>)</b>	1.572
<b>μ (mm<sup>-1</sup>)</b>	1.135
<b>F (000)</b>	936

<b>Radiation</b>	MoK $\alpha$ ( $\lambda = 0.71073$ )
<b>2<math>\theta</math> range for data collection (°)</b>	4.482 to 54.196
<b>Index ranges</b>	-21 $\leq h \leq$ 21 -13 $\leq k \leq$ 13 -13 $\leq l \leq$ 13
<b>Reflections collected</b>	63288
<b>Independent reflections</b>	4336 [ $R_{\text{int}} = 0.0421$ , $R_{\text{sigma}} = 0.0160$ ]
<b>Data/restraints/parameters</b>	4336/1/245
<b>Goodness of fit on <math>F^2</math></b>	1.125
<b>Final R indexes [<math>I &gt; 2\sigma(I)</math>]</b>	$R_1 = 0.0153$ , $wR_2 = 0.0355$
<b>Final R indexes [all data]</b>	$R_1 = 0.0175$ , $wR_2 = 0.0377$
<b>Largest diff. peak/hole/ (<math>\text{\AA}^{-3}</math>)</b>	0.24/-0.42
<b>Flack parameter</b>	0.09(2)
<b>CSD number</b>	2006488

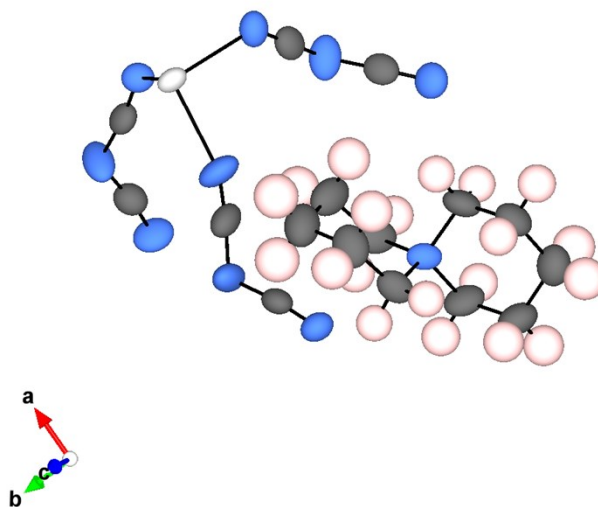


**Figure S10:** Structure of the  $ABX_3$  repetition unit of the  $[ASU][Cd(C_2N_3)_3]$  compound shown as displacement ellipsoids with 90% probability. The  $(C_2N_3)^-$  ligands act as bridges between the  $Cd^{2+}$  cations and the  $[ASU]^+$  cations are located in the void of the pseudocubic  $ReO_3$ -type cavities. Colour code: Cd – light grey, N – blue, C – dark grey, H – light pink.

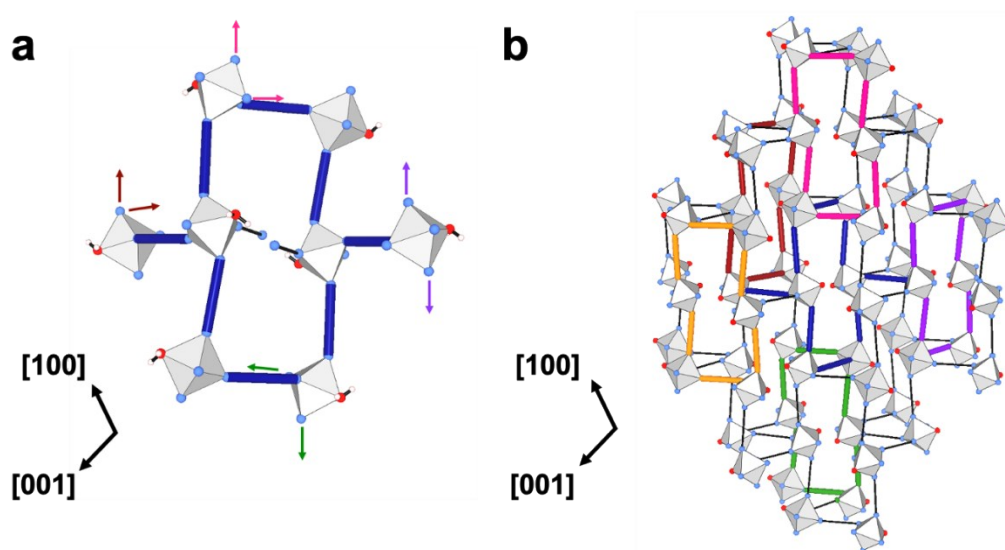
**Table S3:** Crystallographic data from SCXRD for the [ASU]<sub>2</sub>[Ni<sub>2</sub>(C<sub>2</sub>N<sub>3</sub>)<sub>6</sub>·2H<sub>2</sub>O] compound at 100 K.

<b>Compound</b>	[ASU] <sub>2</sub> [Ni <sub>2</sub> (C <sub>2</sub> N <sub>3</sub> ) <sub>6</sub> ·2H <sub>2</sub> O
<b>Chemical Formula</b>	C <sub>32</sub> H <sub>44</sub> N <sub>20</sub> Ni <sub>2</sub> O <sub>2</sub>
<b>Formula weight (g/mol)</b>	858.29
<b>Temperature (K)</b>	100
<b>Crystal system</b>	monoclinic
<b>Space group</b>	<i>P2<sub>1</sub>/n</i>
<b>a (Å)</b>	20.3343(9)
<b>b (Å)</b>	9.9398(5)
<b>c (Å)</b>	20.5387(10)
<b>α (°)</b>	90
<b>β (°)</b>	106.735(2)
<b>γ (°)</b>	90
<b>Volume (Å<sup>3</sup>)</b>	3975.4(3)
<b>Z</b>	4
<b>ρ<sub>calc</sub> (g/cm<sup>3</sup>)</b>	1.434
<b>μ (mm<sup>-1</sup>)</b>	1.005
<b>F (000)</b>	1792.0
<b>Radiation</b>	MoK <sub>α</sub> (λ = 0.71073)
<b>2θ range for data collection (°)</b>	4.066 to 52.744
<b>Index ranges</b>	-25 ≤ h ≤ 25 -12 ≤ k ≤ 12 -25 ≤ l ≤ 25
<b>Reflections collected</b>	185958
<b>Independent reflections</b>	8144 [R <sub>int</sub> = 0.0626, R <sub>sigma</sub> = 0.0173]
<b>Data/restraints/parameters</b>	8144/0/491
<b>Goodness of fit on F<sup>2</sup></b>	1.080
<b>Final R indexes [I &gt; 2σ (I)]</b>	R <sub>1</sub> = 0.0477, wR <sub>2</sub> = 0.1030
<b>Final R indexes [all data]</b>	R <sub>1</sub> = 0.0588, wR <sub>2</sub> = 0.1130
<b>Largest diff. peak/hole/ (Å<sup>-3</sup>)</b>	0.69/-0.61
<b>CSD number</b>	2006489

### Single crystal structure of non-perovskite coordination networks:

For the smaller divalent B-site cations ( $B = \text{Mn}^{2+}$ ,  $\text{Co}^{2+}$ , and  $\text{Ni}^{2+}$ ), isostructural diamond-type coordination networks with the general formula  $[\text{ASU}]_2[\text{B}_2(\text{C}_2\text{N}_3)]_6 \cdot 2\text{H}_2\text{O}$  could be obtained. The  $\text{Mn}^{2+}$ ,  $\text{Co}^{2+}$  and  $\text{Ni}^{2+}$  compounds crystallise in the monoclinic centrosymmetric space-group  $P2_1/n$ . The underlying topology of the crystal structure was determined with TopCryst.<sup>8</sup>

**Figure S11:** The structure of the coordination networks  $[\text{ASU}]_2[\text{B}_2(\text{C}_2\text{N}_3)]_6 \cdot 2\text{H}_2\text{O}$  ( $B = \text{Mn}^{2+}$ ,  $\text{Co}^{2+}$  and  $\text{Ni}^{2+}$ ) exemplary shown with the Ni compound. (a) shows the repeating motif formed of  $\text{B}^{2+}$  and  $(\text{C}_2\text{N}_3)^-$  bridging ligands. (b) The supercell  $2 \times 2 \times 2$  for a schematic representation of the unusual network connectivity. The repeating unit of (a) is shown in the middle (dark blue) and individual rings consists of six linked  $\text{BN}_5\text{O}$  octahedrons that display two corners at the same time.  $[\text{ASU}]^+$  cations, C atoms and H atoms in (b) were removed for better visualisation of the structure. Colour code: B – light grey, O – red, H – white, N – light blue.



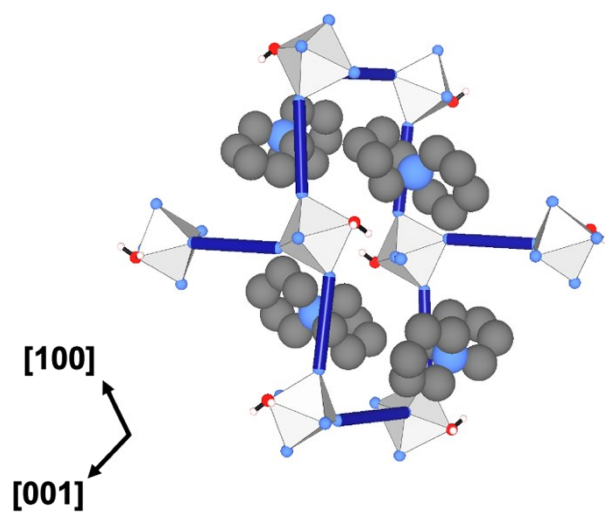


**Figure S12:** Visualisation of the dominating motif shown with the Ni compound and with [ASU]<sup>+</sup> cations for charge balance. For a better demonstration, the non-bridging  $\mu_{1,5}$ -dca linkers and the C atoms of the ligand were removed. Colour code: Ni – light grey, O – red, H – white, N – light blue, C – dark grey.

## Group theoretical analysis

Group-theoretical analysis was carried out by the web-based software ISODISTORT.<sup>9</sup> The structure was simplified by removing the A-site cation and the software FINDSYM<sup>10</sup> was used to verify that the omission of the cation did not change the symmetry. The modified structure was decomposed relative to a hypothetical parent perovskite structure with symmetry  $Pm\bar{3}m$  and linear linker. The origin was located on the A-site; note that the exact irrep label depends on the origin choice. Details of the results including magnitude are given in Table S4.

**Table S4:** Group theoretical analysis of [ASU][Cd(C<sub>2</sub>N<sub>3</sub>)<sub>3</sub>]. The four strongest irreps are listed in order of decreasing magnitude. It shows the irrep, its relative magnitude, its order parameter direction, the space group it would give to if acting in isolation and a description. The primary order parameters (the set of distortions fully accounting for the symmetry) with largest magnitude are M<sub>2</sub><sup>-</sup>, R<sub>5</sub><sup>-</sup> and M<sub>5</sub><sup>+</sup>.

Irrep	Order parameter direction	Space group	Description
M <sub>2</sub> <sup>-</sup>	(a;0;0)	<i>P4/nmm</i>	Checkerboard shift
R <sub>5</sub> <sup>-</sup>	(0,a,a)	<i>Imma</i>	Out-of-phase conv. tilt
X <sub>5</sub> <sup>+</sup>	(0,0;0,0;a,a)	<i>Cmcm</i>	Dicyanamide bending
M <sub>5</sub> <sup>+</sup>	(a,-a;0,0;0,0)	<i>Pmna</i>	Unconventional tilts

## Second Harmonic Generation studies

Assessment of SHG efficiency of  $[\text{ASU}]\text{Cd}(\text{C}_2\text{N}_3)_3$  was performed with the use of Kurtz-Perry technique.

Generally, Kurtz-Perry technique requires the use of size-graded crystalline samples. Potassium dihydrogen phosphate (KDP) was used as a SHG reference.<sup>11,12</sup> Thus, prior to measurements, the single crystals of  $[\text{ASU}]\text{Cd}(\text{C}_2\text{N}_3)_3$  and KDP were crushed with spatula and sieved through a mini-sieve set (Aldrich), collecting a microcrystal size fraction of 88 - 125  $\mu\text{m}$ . Next, size-graded samples of  $[\text{ASU}]\text{Cd}(\text{C}_2\text{N}_3)_3$  and KDP were fixed between microscope glass slides forming tightly packed layers, sealed, and mounted to holder. Kurtz-Perry test was performed at 293K. As seen in Fig. S13, strong SHG signal at 400 nm was registered for  $[\text{ASU}]\text{Cd}(\text{C}_2\text{N}_3)_3$ , unequivocally confirming its non-centrosymmetric structure. Under identical irradiation conditions the SHG signal was collected from the KDP powder of the same particle size. The ratio of integral intensities of SHG signals demonstrates that the relative SHG efficiency of  $[\text{ASU}]\text{Cd}(\text{C}_2\text{N}_3)_3$  is equal to 0.21 that of KDP at 293K.

The laser radiation was delivered from a *Quantronix Integra-C* regenerative amplifier operating at 800 nm, pulse duration of 130 fs, and repetition rate of 1 kHz. The laser beam was passed through 5 mm aperture and was directed onto  $[\text{ASU}]\text{Cd}(\text{C}_2\text{N}_3)_3$  and KDP samples at 45 degrees. Laser beam was unfocused and its mean power was equal to 86 mW. Signal-collecting optics, mounted to the glass optical fiber, was placed perpendicularly to the plane of sample (backscattering geometry). Scattered pumping radiation was suppressed with the use of 700 nm shortpass dielectric filter (FESH0700, Thorlabs). The spectra of the diffused SHG were recorded by an *Ocean Optics Flame T fiber-coupled* CCD spectrograph (200  $\mu\text{m}$  entrance slit).

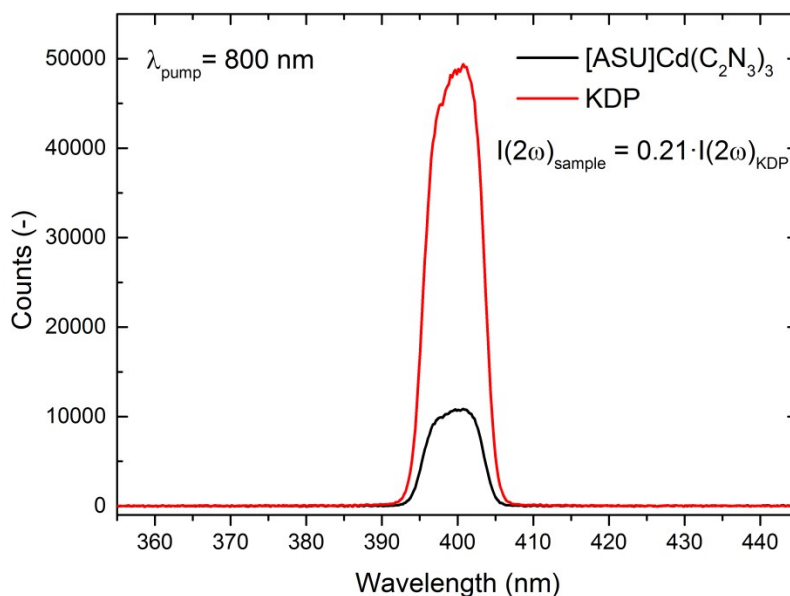


**Figure S13:** A comparison of SHG traces for  $[\text{ASU}]\text{Cd}(\text{C}_2\text{N}_3)_3$  (black) and that of KDP (red). The collection time of SHG signals for both,  $[\text{ASU}]\text{Cd}(\text{C}_2\text{N}_3)_3$  and KDP, was equal to 6000 ms. Powders of both compounds were sieved into 88 - 125  $\mu\text{m}$  particle size range.

## References

1. M. G. Marino and K. D. Kreuer, *ChemSusChem*, 2015, **8**, 513.
2. G. R. Fulmer, A. J. M. Miller, N. H. Sherden, H. E. Gottlieb, A. Nudelman, B. M. Stoltz, J. E. Bercaw and K. I. Goldberg, *Organometallics*, 2010, **29**, 2176.
3. APEX suite of crystallographic software, *APEX 2 Version 2008.4*, Bruker AXS Inc., Madison, WI, USA, 2008.
4. SAINT, *Version 7.56a*, Bruker AXS Inc., Madison, WI, USA, 2008.
5. SADABS, *Version 2008/1*, Bruker AXS Inc., Madison, WI, USA, 2008.
6. G. M. Sheldrick, *Acta crystallographica. Section A, Foundations of crystallography*, 2008, **64**, 112.
7. O. V. Dolomanov, L. J. Bourhis, R. J. Gildea, J. A. K. Howard and H. Puschmann, *J Appl Crystallogr*, 2009, **42**, 339.
8. V. A. Blatov, A. P. Shevchenko and D. M. Proserpio, *Cryst. Growth Des.*, 2014, **14**, 3576.
9. B. J. Campbell, H. T. Stokes, D. E. Tanner and D. M. Hatch, *J. Appl. Crystallogr.*, 2006, **39**, 607.
10. H. T. Stokes and D. M. Hatch, *J. Appl. Crystallogr.*, 2005, **38**, 237.
11. S. K. Kurtz and T. T. Perry, *Journal of Applied Physics*, 1968, **39**, 3798.
12. A. Graja, *Phys. Stat. Sol. (b)*, 1968, **27**, K93-K97.